Author disclosures are available with the text of this letter at www.atsjournals.org.

Anne-Fleur Haudebourg, M.D.
François Perier, M.D.
Samuel Tuffet, M.D.
Nicolas de Prost, M.D., Ph.D.
Keyvan Razazi, M.D.
Armand Mekontso Dessap, M.D., Ph.D.
CHU Henri Mondor
Créteil, France
and
Université Paris Est-Créteil
Créteil, France

Guillaume Carteaux, M.D., Ph.D.*
CHU Henri Mondor
Créteil, France
Université Paris Est-Créteil
Créteil, France
and
Institut Mondor de Recherche Biomédicale INSERM 955
Créteil, France

*Corresponding author (e-mail: guillaume.carteaux@aphp.fr).

References

1. Yang X, Yu Y, Xu J, Shu H, Xia J, Liu H, *et al*. Clinical course and outcomes of critically ill patients with SARS-CoV-2 pneumonia in Wuhan, China: a single-centered, retrospective, observational study. *Lancet Respir Med* 2020;8:475–481.
2. Grasselli G, Zangrillo A, Zanella A, Antonelli M, Cabrini L, Castelli A, *et al*.; COVID-19 Lombardy ICU Network. Baseline characteristics and outcomes of 1591 patients infected with SARS-CoV-2 admitted to ICUs of the Lombardy Region, Italy. *JAMA* 2020;323: 1574–1581.
3. Gattinoni L, Coppola S, Cressoni M, Busana M, Rossi S, Chiumello D. Covid-19 does not lead to a "typical" acute respiratory distress syndrome. *Am J Respir Crit Care Med* 2020;201:1299–1300.
4. Tobin MJ. Basing respiratory management of COVID-19 on physiological principles [editorial]. *Am J Respir Crit Care Med* 2020; 201:1319–1320.
5. Gattinoni L, Chiumello D, Caironi P, Busana M, Romitti F, Brazzi L, *et al*. COVID-19 pneumonia: different respiratory treatments for different phenotypes? *Intensive Care Med* [online ahead of print] 14 Apr 2020; DOI: 10.1007/s00134-020-06033-2.
6. Pan C, Chen L, Lu C, Zhang W, Xia J-A, Sklar MC, *et al*.. Lung recruitability in COVID-19-associated acute respiratory distress syndrome: a single-center observational study. *Am J Respir Crit Care Med* 2020;201:1294–1297.
7. Ranieri VM, Rubenfeld GD, Thompson BT, Ferguson ND, Caldwell E, Fan E, *et al*.; ARDS Definition Task Force. Acute respiratory distress syndrome: the Berlin definition. *JAMA* 2012;307: 2526–2533.
8. Chen L, Del Sorbo L, Grieco DL, Junhasavasdikul D, Rittayamai N, Soliman I, *et al*. Potential for lung recruitment estimated by the recruitment-to-inflation ratio in acute respiratory distress syndrome: a clinical trial. *Am J Respir Crit Care Med* 2020;201: 178–187.
9. Brochard L, Slutsky A, Pesenti A. Mechanical ventilation to minimize progression of lung injury in acute respiratory failure. *Am J Respir Crit Care Med* 2017;195:438–442.
10. Simonnet A, Chetboun M, Poissy J, Raverdy V, Noulette J, Duhamel A, *et al*.; Lille Intensive Care COVID-19 and Obesity study group. High prevalence of obesity in severe acute respiratory syndrome coronavirus-2 (SARS-CoV-2) requiring invasive mechanical ventilation. *Obesity (Silver Spring)* [online ahead of print] 9 Apr 2020; DOI: 10.1002/oby.22831.
11. Grieco DL, Chen L, Brochard L. Transpulmonary pressure: importance and limits. *Ann Transl Med* 2017;5:285.

Regional Structure-Function in Cystic Fibrosis Lung Disease Using Hyperpolarized ^{129}Xe and Ultrashort Echo Magnetic Resonance Imaging

To the Editor:

Cystic fibrosis (CF) is a genetic disorder that exhibits a number of different structural pulmonary abnormalities such as mucus plugs (MP), bronchiectasis (BR), bronchial wall (BW) thickening, and consolidations (CNs), each of which contribute to abnormal ventilation via regional obstruction. Although structural imaging methods (generally X-ray computed tomography [CT]) can depict regional structural pathologies, the precise extent to which these structural abnormalities contribute to lung function decline is not well understood. Here, we demonstrate that hyperpolarized (HP) gas magnetic resonance imaging (MRI) can be combined with ultrashort echo (UTE) MRI (a radiation-free alternative to CT [1–3]) to quantify the relationships between individual regional pathologies and regional ventilation (4–6). The aim of this work was to quantify the size and extent of regional ventilation defects in CF using HP ^{129}Xe MRI and to associate these with the presence of specific structural abnormalities identified by UTE MRI: BR, BW thickening, MP, ground-glass opacities, and CN. We hypothesized that low-ventilation regions could be attributed to spatially matched pathologies seen in UTE images.

Methods

A total of five healthy control subjects (mean ± SD age, 10.8 ± 3.9 yr) and 22 clinically stable patients with CF (age, 14.5 ± 10.6 yr) were imaged under an Institutional Review Board–approved protocol, with a Food and Drug Administration Investigational New Drug (123577) for ^{129}Xe; informed consent was obtained from adult subjects or parents, and age-appropriate assent from pediatric subjects (demographic data in Table 1). Spirometry was obtained in each subject before imaging according to American Thoracic Society and European Respiratory Society guidelines. Subjects were imaged on a Philips 3T Achieva (Philips Healthcare) by coaching subjects to FRC before inhalation of a breath of

Supported by NIH grants T32 HL007752, R01 HL131012, and R44HL123299.

Author Contributions: Concept and design: R.P.T., L.L.W., D.J.R., N.H., A.S., A.B., J.P.C., Z.I.C., and J.C.W. Data acquisition: R.P.T., L.L.W., D.J.R., N.H., Z.I.C., and J.C.W. Image analysis: R.P.T. and J.C.W. Radiological interpretation: A.S. and A.B. Interpretation of results: R.P.T., L.L.W., D.J.R., N.H., A.S., A.B., J.P.C., Z.I.C., and J.C.W. All authors contributed to the intellectual content of this manuscript.

Originally Published in Press as DOI: 10.1164/rccm.202001-0031LE on April 3, 2020

Table 1. Individual Subject Demographic Data and Spirometry/VDP Results

Subject Number	Age (*yr*)	Sex	Height (*cm*)	CF Genotype	$ppFEV_1$ (%)	VDP (%)
1	16	F	169	Control	110	0.8
2	12	M	160	Control	92	1.0
3	12	M	141	Control	103	1.5
4	6	F	116	Control	95	2.0
5	6	M	116.4	ΔΔF508	100	2.3
6	6	M	112	ΔΔF508	99	2.7
7	8	M	136	Control	91	2.8
8	7	M	109.9	ΔΔF508	116	3.9
9	6	F	105.2	ΔΔF508	97	5.4
10	11	F	149.9	ΔΔF508	119	6.1
11	6	M	121	ΔF508/R560T	81	8.6
12	11	F	147	ΔΔF508	86	8.8
13	11	F	152	ΔΔF508	89	9.0
14	13	M	146	$3120^{+}1G>$ A/$3120^{+}1G>A$	78	9.2
15	12	M	158.6	ΔF508/W1282X	89	9.4
16	46	M	165	ΔΔF508	83	15.9
17	6	M	119	ΔΔF508	74	16.5
18	11	F	144.1	ΔΔF508	87	18.1
19	9	F	132.1	ΔΔF508	101	19.8
20	8	M	120.7	ΔΔF508	88	19.9
21	16	F	153	$3849/849^{+}$ 10kbC>T	61	21.4
22	11	M	142	F508del/ R1066H	102	22.8
23	16	F	159	ΔΔF508	72	23.9
24	19	F	163	ΔΔF508	66	25.6
25	26	F	157	ΔΔF508	78	26.8
26	26	M	175	F508del/G551D	39	33.8
27	37	F	151.5	F508del/S945L	38	44.0

Definition of abbreviations: CF = cystic fibrosis; $ppFEV_1$ = percent predicted FEV_1; VDP = ventilation defect percentage.

HP ^{129}Xe (one-sixth TLC, based on height and sex [7]) for ventilation imaging via a gradient-echo sequence (two-dimensional multislice, TR/TE = 8/4 ms; voxel size = $3 \times 3 \times 15$ mm^3; readouts = 96–196; phase encodes = 50–64; FA = 9–12°; and slices = 9–15). UTE magnetic resonance images were acquired during resting breathing, gated to FRC, with a 32-channel proton cardiac phased-array coil (radial three-dimensional stack-of-stars sequence, 40,000 projections, TE = 0.2 ms, TR = 4.8–6.2 ms, FA = 5°, voxel size = 1.19–1.45 mm^2 in-plane resolution, slice thickness = 4 mm, and bandwidth ≈ 1.8 kHz). ^{129}Xe signal intensity was normalized to the whole-lung HP gas signal mean and lung voxels with ^{129}Xe signal <60% of the whole-lung signal were identified as defects (8, 9). The percentage of an individual's lung volume identified as defect is quantified as the subject's ventilation defect percentage (VDP). UTE magnetic resonance images were visually analyzed independently by two radiologists (A.S. and A.B.) for regions of structural abnormality: BR, BW thickening, MP, CN, and ground-glass opacities. The identified abnormalities were then visually matched to corresponding regions in the HP ^{129}Xe MRI to associate the identified structural abnormalities with corresponding ventilation defects (Figure 1). Radiologists also assigned an integer quality score between 1 and 5 (low and high, respectively) to each subject's UTE dataset, which were averaged to provide an overall image quality score.

Results

Table 1 shows individual results for FEV_1 and VDP. Average FEV_1 was 98.2% ± 8.1% for controls and 83.8% ± 20.6% for subjects with CF ($P = 0.02$). Average VDP was 1.6% ± 0.8% for control subjects and 16.1% ± 10.8% for patients with CF ($P < 10^{-5}$). Of the total calculated ^{129}Xe defect volume across all subjects, only 50.6% was associated with a spatially matched structural abnormality from UTE MRI. Of the calculated ^{129}Xe defect volumes that were associated to structural abnormalities, 76.8% were associated with BR and/or BW thickening and 76.6% were associated with MP, with significant overlap in attribution (only 16.2% and 17.9% exclusively associated with BR/BW and MP, respectively). Individual subject counts of structural abnormalities correlated strongly with VDPs (Pearson $r = 0.81$; $P < 10^{-6}$) but only moderately with FEV_1 ($r = -0.68$; $P = 0.0001$), as expected. Pearson correlation was $r = -0.78$ ($P < 10^{-5}$) between subject VDP and FEV_1.

Discussion

This work presents the first direct quantification of ^{129}Xe ventilation impairment associated with specific regional structural abnormalities in CF lung disease. BR and MP were responsible for the vast majority of structurally attributed defects, but the large quantity of defects that could not be associated with structural abnormalities underscores the sensitivity of ^{129}Xe MRI to mild obstruction. The lower resolution inherent to UTE MRI (here, ~1.2 mm) may have resulted in undetectable small structural abnormalities that would have been detected with high-resolution CT (0.4 mm). X-ray CT remains the gold standard for structural imaging, especially with respect to quantitative assessment of airways and reduced lung parenchymal density on expiration, associated with air trapping. However, this further highlights ^{129}Xe MRI as a sensitive technique for evaluating and quantifying regional lung function, particularly in cases in which structural imaging alone yields inconclusive results and in mild disease, in which functional declines are subclinical. This combination of MRI techniques may be beneficial in the future to aid clinical decision-making, particularly in evaluation of individual patient outcomes, in which repeated testing is useful, and as a biomarker for upcoming clinical trials. We find that ^{129}Xe MRI often shows ventilation impairment even in the absence of identifiable structural abnormalities, and that within defect regions, ^{129}Xe signal is greater if no structural abnormality could be regionally matched from structural imaging. This highlights ^{129}Xe imaging as a sensitive tool for pulmonary research and may be clinically useful in the evaluation and/or management of patients with CF in early stages of lung function decline. ■

Author disclosures are available with the text of this letter at www.atsjournals.org.

Robert P. Thomen, Ph.D.
University of Missouri
Columbia, Missouri

Laura L. Walkup, Ph.D.
Cincinnati Children's Hospital Medical Center
Cincinnati, Ohio
and
University of Cincinnati
Cincinnati, Ohio

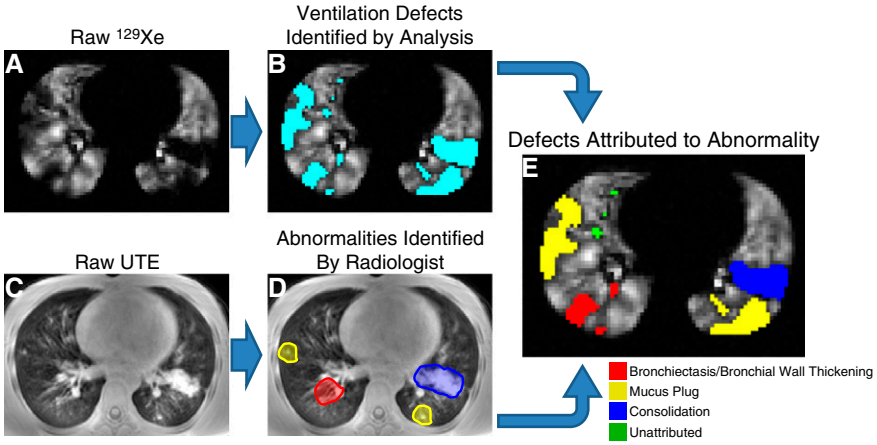

Figure 1. Example of image analysis pipeline shown in a patient with cystic fibrosis (subject 22). (*A* and *C*) ^{129}Xe and ultrashort echo (UTE) magnetic resonance images are collected in the same imaging session, respectively. (*B* and *D*) Ventilation defects are quantified in the ^{129}Xe magnetic resonance imaging (*B*, defects colored cyan) and abnormalities are independently identified within the UTE by trained readers (*D*). (*E*) ^{129}Xe defects are separately associated with proximal or adjacent structural abnormalities for quantitative analysis.

David J. Roach, Ph.D.
Nara Higano, Ph.D.
Andrew Schapiro M.D.
Alan Brody, M.D.
Cincinnati Children's Hospital Medical Center
Cincinnati, Ohio

John P. Clancy, M.D.
Zackary I. Cleveland, Ph.D.
Jason C. Woods, Ph.D.*
Cincinnati Children's Hospital Medical Center
Cincinnati, Ohio
and
University of Cincinnati
Cincinnati, Ohio

ORCID ID: 0000-0002-5060-6401 (L.L.W.).

*Corresponding author (e-mail: jason.woods@cchmc.org).

References

1. Roach DJ, Crémillieux Y, Serai SD, Thomen RP, Wang H, Zou Y, *et al*. Morphological and quantitative evaluation of emphysema in chronic obstructive pulmonary disease patients: a comparative study of MRI with CT. *J Magn Reson Imaging* 2016;44:1656–1663.
2. Dournes G, Grodzki D, Macey J, Girodet PO, Fayon M, Chateil JF, *et al*. Quiet submillimeter MR imaging of the lung is feasible with a PETRA sequence at 1.5 T. *Radiology* 2015;276:258–265.
3. Higano NS, Fleck RJ, Spielberg DR, Walkup LL, Hahn AD, Thomen RP, *et al*. Quantification of neonatal lung parenchymal density via ultrashort echo time MRI with comparison to CT. *J Magn Reson Imaging* 2017;46:992–1000.
4. Wielpütz MO, Puderbach M, Kopp-Schneider A, Stahl M, Fritzsching E, Sommerburg O, *et al*. Magnetic resonance imaging detects changes in structure and perfusion, and response to therapy in early cystic fibrosis lung disease. *Am J Respir Crit Care Med* 2014; 189:956–965.
5. Roach DJ, Crémillieux Y, Fleck RJ, Brody AS, Serai SD, Szczesniak RD, *et al*. Ultrashort echo-time magnetic resonance imaging is a sensitive method for the evaluation of early cystic fibrosis lung disease. *Ann Am Thorac Soc* 2016;13:1923–1931.
6. Stahl M, Wielpütz MO, Graeber SY, Joachim C, Sommerburg O, Kauczor HU, *et al*. Comparison of lung clearance index and magnetic resonance imaging for assessment of lung disease in children with cystic fibrosis. *Am J Respir Crit Care Med* 2017;195: 349–359.
7. Zapletal A, Paul T, Samánek M. Significance of contemporary methods of lung function testing for the detection of airway obstruction in children and adolescents (author's translation) [in German]. *Z Erkr Atmungsorgane* 1977;149:343–371.
8. Thomen RP, Sheshadri A, Quirk JD, Kozlowski J, Ellison HD, Szczesniak RD, *et al*. Regional ventilation changes in severe asthma after bronchial thermoplasty with (3)He MR imaging and CT. *Radiology* 2015;274:250–259.
9. Thomen RP, Walkup LL, Roach DJ, Cleveland ZI, Clancy JP, Woods JC. Hyperpolarized ^{129}Xe for investigation of mild cystic fibrosis lung disease in pediatric patients. *J Cyst Fibros* 2017;16:275–282.

Factors Associated with Low Lung Function in Different Age Bins in the General Population

To the Editor:

There is a range of lung function trajectories throughout life (1–3), some of which are associated with significant morbidity and premature mortality (4, 5). They are the end result of gene–environment interactions that start *in utero* and continue after birth until death (6, 7), but their relationships in different

Supported by the National Scientific Grant 2018 from the Austrian Society for Pneumology. The Austrian LEAD Study is supported by the Ludwig Boltzmann Society, the Municipal Department of Health and Environment of Vienna, the Federal State Governmental Department of Health of Lower Austria, and unrestricted scientific grants from Astra Zeneca, Böhringer Ingelheim, Chiesi Pharma, GlaxoSmithKline, Menarini Pharma, MSD, Novartis Pharma, and Teva. R.F. is the recipient of an Instituto de Salud Carlos III research contract (CP16/00039). None of the supporting parties participated in data collection or analysis, or contributed to the design of the study or the content of the manuscript.

Originally Published in Press as DOI: 10.1164/rccm.202001-0172LE on April 7, 2020